© 2014. Published by The Company of Biologists Ltd | Development (2014) 141, 1857-1863 doi:10.1242/dev.104224

RESEARCH REPORT

CXCR7 prevents excessive CXCL12-mediated downregulation of CXCR4 in migrating cortical interneurons

Philipp Abe[1,*], Wiebke Mueller[1,*], Dagmar Schütz[1], Fabienne MacKay[2], Marcus Thelen[3], Penglie Zhang[4] and Ralf Stumm[1,‡]

ABSTRACT

The CXCL12/CXCR4 signaling pathway is involved in the development of numerous neuronal and non-neuronal structures. Recent work established that the atypical second CXCL12 receptor, CXCR7, is essential for the proper migration of interneuron precursors in the developing cerebral cortex. Two CXCR7-mediated functions were proposed in this process: direct modulation of β-arrestin-mediated signaling cascades and CXCL12 scavenging to regulate local chemokine availability and ensure responsiveness of the CXCL12/CXCR4 pathway in interneurons. Neither of these functions has been proven in the embryonic brain. Here, we demonstrate that migrating interneurons efficiently sequester CXCL12 through CXCR7. CXCR7 ablation causes excessive phosphorylation and downregulation of CXCR4 throughout the cortex in mice expressing CXCL12, but not in CXCL12-deficient animals. *Cxcl12*$^{-/-}$ mice lack activated CXCR4 in embryonic brain lysates and display a similar interneuron positioning defect as *Cxcr4*$^{-/-}$, *Cxcr7*$^{-/-}$ and *Cxcl12*$^{-/-}$;*Cxcr7*$^{-/-}$ animals. Thus, CXCL12 is the only CXCR4-activating ligand in the embryonic brain and deletion of one of the CXCL12 receptors is sufficient to generate a migration phenotype that corresponds to the CXCL12-deficient pathway. Our findings imply that interfering with the CXCL12-scavenging activity of CXCR7 causes loss of CXCR4 function as a consequence of excessive CXCL12-mediated CXCR4 activation and degradation.

KEY WORDS: CXCL12, CXCR4, CXCR7 (ACKR3), Interneuron migration, Atypical chemokine receptor, Cortical development, Mouse, Cajal-Retzius cell

INTRODUCTION

The chemokine CXCL12 regulates cell migration and homing processes in the immune system, hematopoietic system, brain, and other tissues (Stumm and Hollt, 2007; Miller et al., 2008; Tiveron and Cremer, 2008; Lewellis and Knaut, 2012). It mediates its effects through canonical G protein-coupled CXCR4 and through CXCR7 (Bleul et al., 1996; Oberlin et al., 1996; Balabanian et al., 2005; Burns et al., 2006). The latter is also referred to as atypical chemokine receptor 3 (ACKR3) because it does not signal through G proteins and elicits no chemotaxis (Thelen and Thelen, 2008). Instead, CXCR7 sequesters CXCL12 from the extracellular environment and, thus, functions as a CXCL12 scavenger (Venkiteswaran et al., 2013; Boldajipour et al., 2008; Luker et al., 2010; Naumann et al., 2010; Hoffmann et al., 2012). Like other heptahelical receptors, including CXCR4, CXCR7 is also capable of modulating downstream pathways through β-arrestin (Cheng et al., 2000; Kalatskaya et al., 2009; Rajagopal et al., 2010). Thus, CXCL12 signaling is subject to particularly complicated regulation. Unraveling the underlying mechanisms will facilitate an understanding of CXCL12-mediated cell guidance and the development of new treatment strategies for cell migration disorders.

Defective CXCR4 regulation has recently been implicated in the perturbed intracortical migration of GABAergic interneurons in genetic schizophrenia models (Meechan et al., 2012; Toritsuka et al., 2013). Cortical interneurons originate in the ganglionic eminences in the ventral telencephalon (Anderson et al., 1997; Marín and Rubenstein, 2001; Hernández-Miranda et al., 2010). They seek the cortical marginal zone (MZ) and subventricular/intermediate zone (SVZ/IZ), where their migration depends on CXCL12 emanating from meningeal cells and pyramidal cell progenitors (Tiveron et al., 2006; Tanaka et al., 2009; Sessa et al., 2010; Zarbalis et al., 2012). Most interneurons express both CXCL12 receptors, and interneurons deficient for CXCR4 or CXCR7 display opposite motility defects (Wang et al., 2011). This suggests that distinct CXCR4-dependent and CXCR7-dependent pathways might exist in interneurons: CXCR4 attracts cells towards CXCL12 through a G protein-dependent pathway (Lysko et al., 2011), whereas CXCR7 modulates MAP kinases through β-arrestin (Wang et al., 2011).

Having observed that CXCR7-deficient interneurons display severely reduced CXCR4 levels and loss of CXCR4 function (Sánchez-Alcañiz et al., 2011), we proposed that CXCR7 regulates interneuron migration by preserving CXCR4. This is consistent with the observation that a reduction in CXCR4 disrupts CXCL12-mediated interneuron guidance (Meechan et al., 2012). Given that proper CXCR4 regulation is essential in interneurons, we examined how the two receptors cooperate in this system. We first tested whether the similar interneuron positioning defects in *Cxcr4*$^{-/-}$ and *Cxcr7*$^{-/-}$ mutants (Sánchez-Alcañiz et al., 2011; Wang et al., 2011) reflect a fully CXCL12-defective pathway by assessing interneuron layering in *Cxcr4*$^{-/-}$, *Cxcr7*$^{-/-}$ and *Cxcl12*$^{-/-}$ mice. This showed that inactivation of one of the CXCL12 receptors is sufficient to generate the phenotype observed in mice lacking CXCL12 signaling. We then demonstrated that migrating interneurons sequester CXCL12 through CXCR7, which supports the concept that CXCR7 acts as a CXCL12 scavenger in these cells. Finally, we conducted biochemical and histochemical studies, from which we conclude that loss of CXCR7 leads to excessive CXCL12-mediated activation and downregulation of CXCR4 in interneurons.

[1]Institute of Pharmacology and Toxicology, Jena University Hospital, Friedrich Schiller University Jena, Jena 07747, Germany. [2]Department of Immunology, Monash University, Alfred Medical Research and Education Precinct (AMREP), 89 Commercial Road, Melbourne, Vic 3004, Australia. [3]Institute for Research in Biomedicine, CH-6500 Bellinzona, Switzerland. [4]ChemoCentryx, 850 Maude Avenue, Mountain View, CA 94043, USA.
*These authors contributed equally to this work

‡Author for correspondence (Ralf.Stumm@med.uni-jena.de)

Received 11 October 2013; Accepted 12 March 2014

Development (2014) 141, 1857-1863 doi:10.1242/dev.104224

RESULTS AND DISCUSSION

Cxcl12$^{-/-}$, *Cxcr4*$^{-/-}$ and *Cxcr7*$^{-/-}$ mice display similar interneuron layering defects

To examine whether aberrant interneuron layering in *Cxcr4*$^{-/-}$ and *Cxcr7*$^{-/-}$ mutants corresponds to a partial or complete CXCL12 signaling defect, we examined patterns of *Lhx6* (a marker for MGE-derived interneurons), *Cxcr4* and *Cxcr7* expression in the cortex of E14.5 *Cxcl12*$^{-/-}$, *Cxcr4*$^{-/-}$ and *Cxcr7*$^{-/-}$ mouse embryos by *in situ* hybridization (Fig. 1). Cell counting showed that the numbers of *Lhx6*$^{+}$ and Cxcr4^{+}/Neo^{+} cells were reduced in the MZ and SVZ and increased in the lower cortical plate/subplate (CP/SP) in the three knockout lines compared with control littermates (Fig. 1Ae-g,Ce-g). *Cxcr7*$^{+}$ cells, as counted in *Cxcl12*$^{-/-}$, *Cxcr4*$^{-/-}$ and control littermates (Fig. 1Be,f), exhibited similar abnormal distributions to *Lhx6*$^{+}$ cells and Cxcr4^{+}/Neo^{+} cells in these knockouts. The matching patterns of *Lhx6*, *Cxcr4* and *Cxcr7* were expected because *Lhx6*$^{+}$ cells constitute the main *Cxcr4*- and *Cxcr7*-expressing population in the embryonic cortex (Sánchez-Alcañiz et al., 2011; Wang et al., 2011). We then compared the laminar distribution of *Lhx6*$^{+}$ cells in *Cxcl12*$^{-/-}$, *Cxcr4*$^{-/-}$ and *Cxcr7*$^{-/-}$ mice using ANOVA. This revealed no significant differences, suggesting that deletion of one of the CXCL12 receptors is

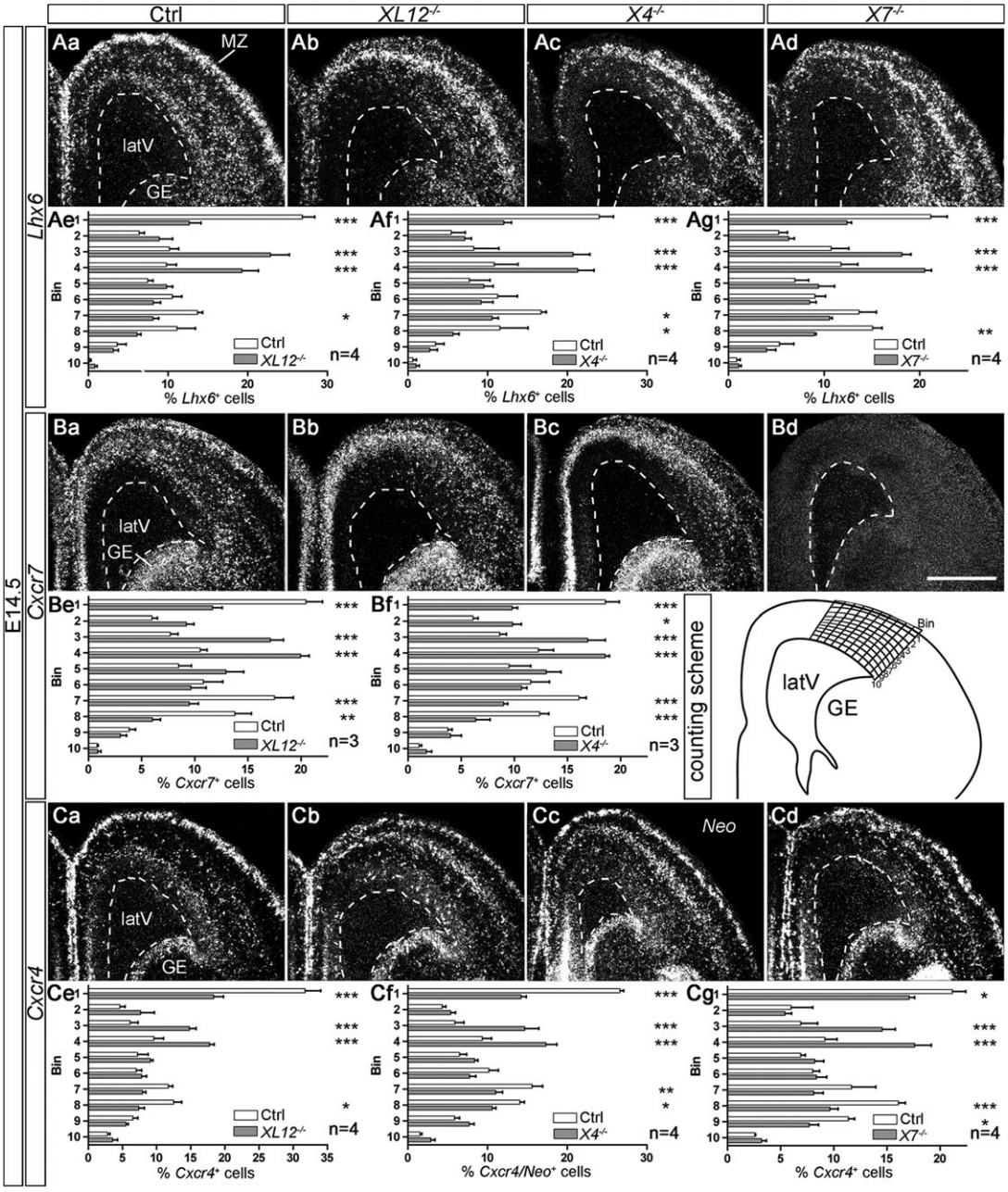

Fig. 1. Similar interneuron distribution defects in E14.5 *Cxcl12*$^{-/-}$, *Cxcr4*$^{-/-}$ and *Cxcr7*$^{-/-}$ mice. Dark-field photographs show the dorsal telencephalon in *in situ* hybridization preparations with ^{35}S-labeled probes for *Lhx6* (Aa-d), *Cxcr7* (Ba-d) and *Cxcr4*/*Neo* (Ca-d) in control (Ctrl), *Cxcl12*$^{-/-}$ (*XL12*$^{-/-}$), *Cxcr4*$^{-/-}$ (*X4*$^{-/-}$) and *Cxcr7*$^{-/-}$ (*X7*$^{-/-}$) mice. The *Neo* probe detects *Cxcr4* gene-derived transcripts in *Cxcr4*$^{-/-}$ mice (Cc). *Cxcr7* transcripts are not detected in *Cxcr7*$^{-/-}$ mutants (Bd). (Ae-g,Be,f,Ce-g) Labeled cells were counted in ten cortical bins (see counting scheme). Proportions per bin (percentage of all counted cells) are presented as mean+s.e.m. Mutants and control littermates were compared using two-way ANOVA and Bonferroni's post-test. *P≤0.05, **P≤0.01 and ***P≤0.001. latV, lateral ventricle; GE, ganglionic eminence; MZ, marginal zone. Scale bar: 500 µm in Bd for Aa-d, Ba-d, Ca-d.

Development (2014) 141, 1857-1863 doi:10.1242/dev.104224

sufficient to generate the interneuron layering defect observed in animals lacking CXCL12.

In the cortex, reelin (*Reln*)$^{+}$ Cajal-Retzius cells represent a second major *Cxcr4*-expressing population that depends on CXCL12/CXCR4 signaling (Stumm et al., 2003; Borrell and Marín, 2006; Paredes et al., 2006). Cell counting in the parietal cortex revealed a reduction of these cells in the MZ (supplementary material Fig. S1A), but only a few ectopic cells in deep cortical layers in *Cxcl12*$^{-/-}$, *Cxcr4*$^{-/-}$ and *Cxcr7*$^{-/-}$ mice. This finding is consistent with the reported function of CXCL12 and CXCR4 in Cajal-Retzius cell dispersion in the MZ (Borrell and Marín, 2006). Given that cortical *Reln*$^{+}$ cells rarely express *Cxcr7* (Schönemeier et al., 2008), our data point to the possibility that CXCR7 exerts some non-autonomous influence on this process.

CXCR7 sequesters CXCL12 in migrating interneurons

By examining red fluorescent protein (RFP) immunoreactivity in the cortex of E14.5 mice expressing CXCL12-RFP fusion protein under the *Cxcl12* promoter (Jung et al., 2009), we identified strongly stained punctae in all cortical layers. The highest densities were observed in the MZ, SP and SVZ/IZ (Fig. 2Aa,B; supplementary material Fig. S1D). This pattern differs markedly from that of *Cxcl12* expression, which is restricted to the meninges and SVZ at E14.5 (Tiveron et al., 2006). Since *Rfp* transcripts in the cortex of CXCL12-RFP embryos faithfully recapitulate the *Cxcl12* mRNA pattern in wild types (supplementary material Fig. S1B), we reasoned that the observed CXCL12-RFP^{+} punctae reflect endocytosed and not nascent CXCL12-RFP. We therefore quantified the number of RFP^{+} punctae (of size >0.5 μm^2) in the cortex of CXCL12-RFP mice lacking the CXCL12 scavenger CXCR7 (Fig. 2Ab). Automated counting using ImageJ revealed a 74.2±9.0% reduction in *Cxcr7*$^{-/-}$;CXCL12-RFP mice as compared with CXCL12-RFP controls (n=4; P<0.01, Student's t-test). Such signal reduction was not observed after *Cxcr4* deletion (Fig. 2Ac). This indicates that most of the strong punctate RFP signal in CXCL12-RFP mice was due to CXCR7-mediated accumulation of CXCL12-RFP. The meninges, in which *Cxcl12* is highly expressed, exhibited similar RFP labeling in receptor-deficient and control mice (supplementary material Fig. S1Ca-c), suggesting that RFP signal in this tissue reflects locally expressed CXCL12-RFP. The specificity of RFP immunostaining was controlled in CXCL12-RFP non-transgenic *Cxcr7*-GFP embryos (supplementary material Fig. S1E).

Closer examination of the RFP pattern in *Cxcr4*$^{-/-}$;CXCL12-RFP sections revealed a signal shift towards the lower CP/SP area (supplementary material Fig. S1D). This aberrant pattern is reminiscent of the interneuron layering defect in *Cxcr4*$^{-/-}$ embryos, suggesting that RFP signal was contained within interneurons. As cortical interneurons do not express *Cxcl12* (Tiveron et al., 2006; Wang et al., 2011), we hypothesized that they sequester CXCL12-RFP. To test this, we generated double-transgenic mice (*Cxcr7*-GFP; CXCL12-RFP) and performed simultaneous live cell imaging of GFP and RFP in E14.5 cortical slices (Fig. 2B; supplementary material Movie 1). Analysis of the confocal images revealed that 96% of *Cxcr7*-GFP^{+} interneurons contained RFP^{+} punctae. To assess whether CXCR7 mediates CXCL12-RFP accumulation in interneurons, we immunostained for RFP in E14.5 *Cxcr7*$^{-/-}$;CXCL12-RFP;*Cxcr7*-GFP and CXCR7-expressing CXCL12-RFP;*Cxcr7*-GFP embryos (Fig. 2Ca-d), and quantified GFP/RFP overlap in the cortex (Mander's coefficient) using ImageJ. In the latter group, 60.3±7.1% of total RFP was present in *Cxcr7*-GFP^{+} interneurons (Fig. 2Ca,b). In the absence of CXCR7, the RFP signal that was contained in *Cxcr7*-GFP^{+}

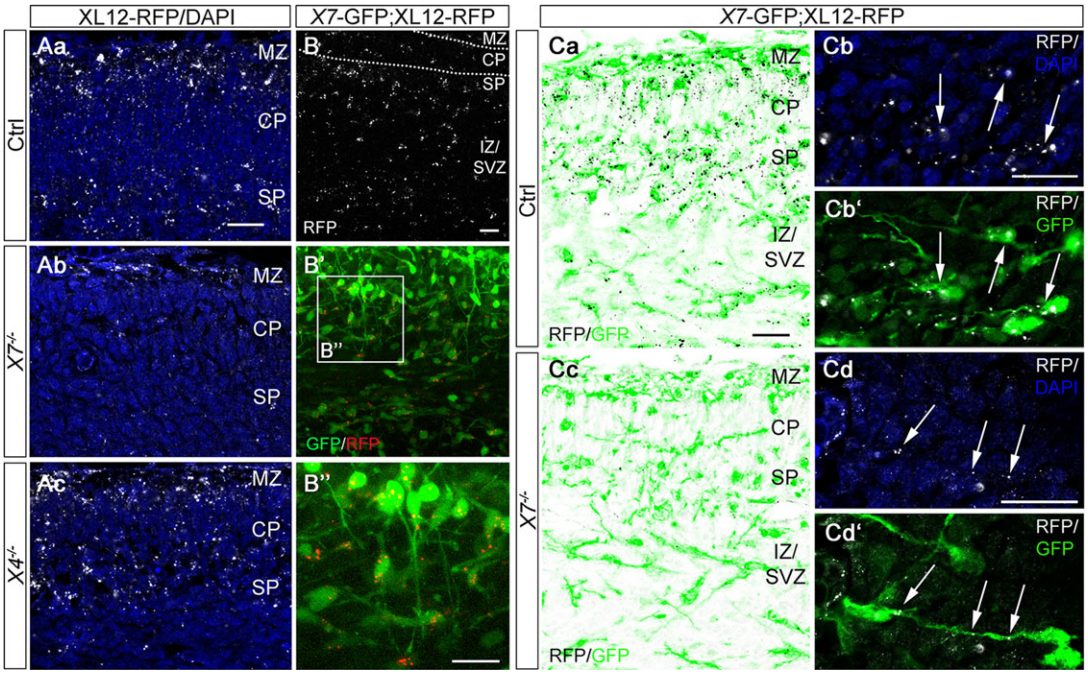

Fig. 2. CXCR7 accumulates CXCL12-RFP in interneurons. Confocal images show RFP in the cortex of E14.5 CXCL12-RFP transgenic mice (XL12-RFP; false colors for RFP are indicated). (A) Immunostained RFP and DAPI in control (Aa), XL12-RFP;*Cxcr7*$^{-/-}$ (*X7*$^{-/-}$, Ab) and XL12-RFP;*Cxcr4*$^{-/-}$ (*X4*$^{-/-}$, Ac) mice. (B-B″) Native RFP (B) and overlay of native GFP/RFP (B′) in a slice from a *Cxcr7*-GFP;XL12-RFP embryo (*X7*-GFP;XL12-RFP). (B″) Magnification of the boxed area in B′ demonstrates RFP^{+} punctae in live GFP^{+} cells. These cells show migration modes characteristic of interneurons (supplementary material Movie 1). (Ca-d) Immunostained RFP in *X7*-GFP;XL12-RFP (Ca,b) and *X7*-GFP;XL12-RFP;*Cxcr7*$^{-/-}$ (Cc,d) mice. Higher magnification images show RFP/DAPI (Cb,d) and RFP/GFP overlays (Cb′,d′). Arrows indicate internalized CXCL12-RFP in *Cxcr7*-GFP+ interneurons. MZ, marginal zone; CP, cortical plate; SP, subplate; IZ/SVZ, intermediate/subventricular zone. Scale bars: 20 μm.

Development (2014) 141, 1857-1863 doi:10.1242/dev.104224

interneurons was decreased by 79.9±7.2% (P<0.0001, Student's t-test; n=4; Fig. 2Cc,d).

We then examined whether *Cxcr7*-GFP^{+} interneurons are capable of internalizing exogenous fluorophore-coupled CXCL12 (CXCL12-565). After validating receptor/CXCL12-565 interaction in transfected HEK293 cells (supplementary material Fig. S2A), we incubated telencephalic slices from E14.5 *Cxcr7*-GFP mice for 30 min with CXCL12-565. CXCL12, the CXCR4 antagonist AMD3100 and the CXCR7 antagonist CCX771 (Zabel et al., 2009) were co-incubated in adjacent slices. Confocal imaging of native fluorescence revealed bright intracellular clusters of CXCL12-565 in *Cxcr7*-GFP^{+} interneurons that received CXCL12-565 alone or CXCL12-565/AMD3100 (supplementary material Fig. S2Ba,c). Slices that received CXCL12-565 and an excess of CXCL12 showed no CXCL12-565 signal, and slices that received CXCL12-565/CCX771 showed faint CXCL12-565 signal, in *Cxcr7*-GFP^{+} interneurons (supplementary material Fig. S2Bb,d). Collectively, our analyses of CXCL12-RFP localization and CXCL12-565 uptake demonstrate that interneurons efficiently internalize CXCL12 via CXCR7.

CXCR7 gauges CXCL12-induced CXCR4 activation in telencephalic cultures

Next, we examined the influence of CXCR7 on CXCL12-induced activation and downregulation of CXCR4 in telencephalic neurons using immunoblots of E14.5 cultures. Blots were reacted with the anti-CXCR4 antibody UMB-2 that recognizes the non-phosphorylated C-terminal epitope 343-352, which undergoes S346/347-phosphorylation upon CXCL12 stimulation (Mueller et al., 2013). Thus, UMB-2 detects inactive CXCR4 in non-dephosphorylated and total CXCR4 in dephosphorylated samples. Consistently, lysate from cultures that received CXCL12 for 30 min showed a strong signal difference between non-dephosphorylated

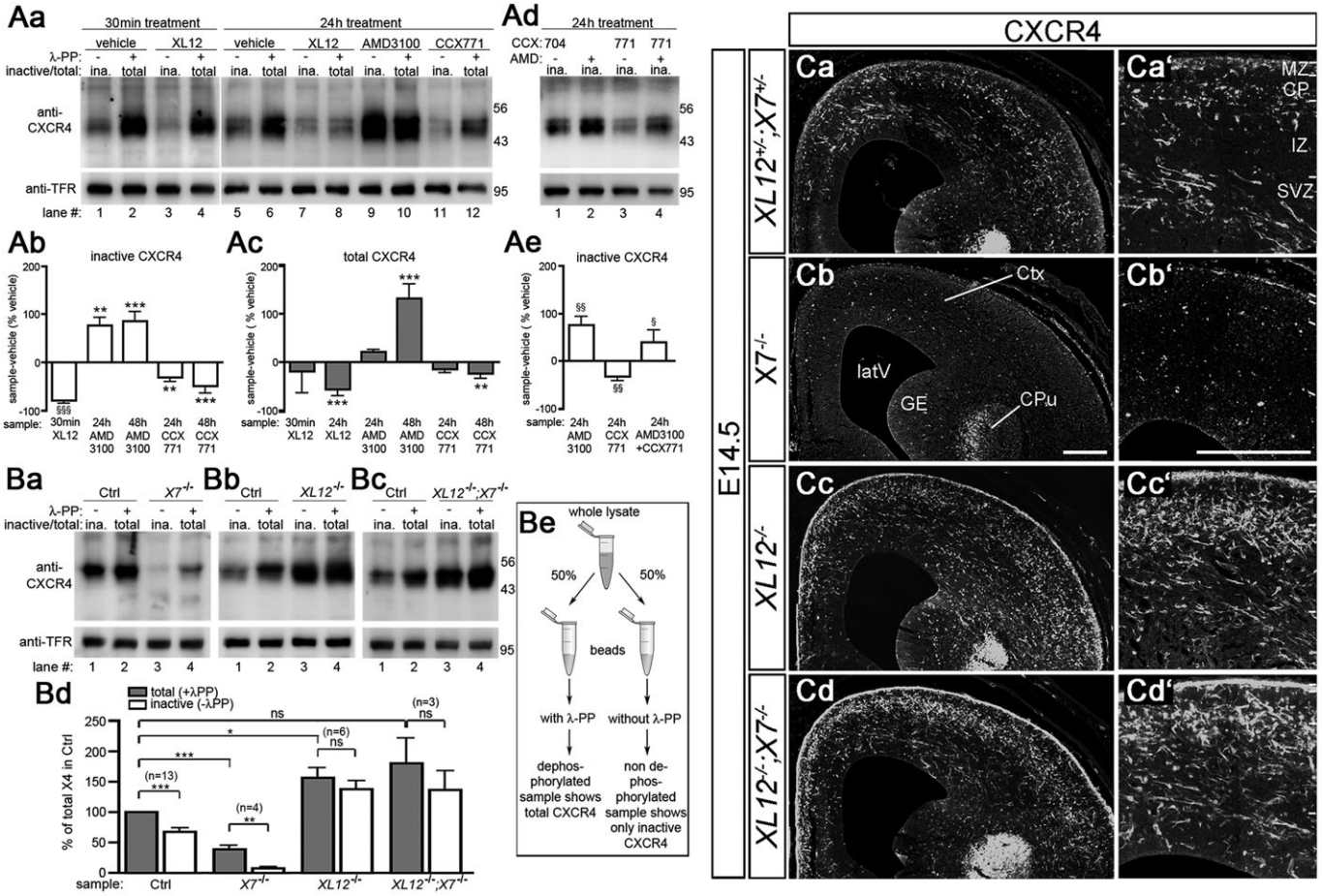

Fig. 3. CXCR7 regulates CXCL12-promoted activation and downregulation of CXCR4. (A,B) Immunoblots analyzing the expression level and activation state of CXCR4 in lysates from E14.5 telencephalic neurons (Aa-e) and E15.5 *Cxcr7*$^{-/-}$ (*X7*$^{-/-}$), *Cxcl12*$^{-/-}$ (*XL12*$^{-/-}$) and *Cxcl12*$^{-/-}$;*Cxcr7*$^{-/-}$ (*XL12*$^{-/-}$;*X7*$^{-/-}$) brains (Ba-d). Blots were reacted with the anti-CXCR4 antibody UMB-2, which detects the non-phosphorylated C-terminus, and with anti-transferrin receptor (TFR) to demonstrate equal loading. (Be) Lysates were split into two aliquots and purified with wheatgerm lectin agarose beads. Aliquots dephosphorylated using Lambda protein phosphatase (λ-PP) show total CXCR4, whereas untreated aliquots show non-phosphorylated/inactive CXCR4 (ina.). (A) CXCL12 (XL12), AMD3100 (AMD), CCX771, and inactive compound (CCX704) were added for the indicated period. (Ab,c,e) For quantification of compound-induced changes in CXCR4, the difference between the UMB-2/TFR signal ratios of compound-treated cultures (sample) and vehicle-treated sister cultures (vehicle) was expressed as a percentage of UMB-2/TFR of the vehicle. Compound-treated and corresponding vehicle-treated groups were compared using one-way ANOVA and Bonferroni's post-test (*) or Student's t-test (§) (three to ten independent repeats). (Ba-c) Immunoblots compare pooled lysates from two knockouts with pooled lysates from two wild-type or heterozygous littermates (Ctrl). (Bd) Each CXCR4/TFR ratio was expressed as a percentage of the CXCR4/TFR ratio of the corresponding λ-PP-treated control before repeats were averaged and analyzed using Student's t-test. Data are mean+s.e.m. $^{*,\S}P\leq0.05$, $^{**,\S\S}P\leq0.01$ and $^{***}P\leq0.001$; ns, not significant. (C) UMB-2 immunofluorescence in coronal head sections of a single E14.5 litter (genotypes as specified in the figure). Higher magnifications (Ca′-d′) show the cerebral cortex. CPu, caudate putamen; GE, ganglionic eminence; latV, lateral ventricle; Ctx, cortex. Scale bars: 200 µm.

Development (2014) 141, 1857-1863 doi:10.1242/dev.104224

and dephosphorylated aliquots, which is characteristic of CXCR4 activation (Fig. 3Aa, lanes 3 and 4). Continuous CXCL12 treatment reduced the CXCR4 level (Fig. 3Aa, lanes 6 and 8; Fig. 3Ac, 24 h XL12), indicating CXCL12-induced CXCR4 downregulation.

Cultures that were maintained over a 24-48 h period without medium exchange exhibited considerable CXCR4 activation (Fig. 3Aa, lanes 5 and 6). Activation was caused by endogenous CXCL12, as 24 h treatment with CXCR4 antagonist (AMD3100) rendered virtually all CXCR4 receptors inactive (Fig. 3Aa, lanes 9 and 10). Continuous antagonist treatment caused an increase in total CXCR4 as compared with vehicle-treated control cultures (Fig. 3Ac, 48 h AMD3100), indicating prevention of CXCL12-induced CXCR4 downregulation. When CXCR7-mediated uptake of endogenous CXCL12 was blocked by long-term CCX771 treatment, CXCR4 levels decreased (Fig. 3Aa, lanes 5, 11 and 6, 12; Fig. 3Ab,c, 24 h and 48 h CCX771). The CCX771 effect was blocked by AMD3100 (Fig. 3Ad, lanes 1, 3, 4; Fig. 3Ae), which suggests that it was CXCL12 mediated. Collectively, these experiments provide evidence that CXCR7 antagonism augments CXCL12-induced activation and downregulation of CXCR4 in telencephalic cultures.

CXCR7 prevents excessive CXCR4 activation by CXCL12

We then assessed whether CXCR7 influences CXCL12-mediated activation and downregulation of CXCR4 in the embryonic brain. We analyzed *Cxcr7*$^{-/-}$, *Cxcl12*$^{-/-}$ and *Cxcl12*$^{-/-}$;*Cxcr7*$^{-/-}$ mice by immunoblotting and immunofluorescence methods. Immunoblots were reacted with UMB-2 (Fig. 3B) and cortical sections with UMB-2 or the phosphorylation-insensitive anti-CXCR4 antibody 2B11 (Fig. 3C; supplementary material Fig. S3A). In all immunoblots, the controls showed a marked difference between total and inactive CXCR4 (Fig. 3Ba-c, lanes 1 and 2; Fig. 3Bd, total versus inactive in control group), indicating substantial CXCR4 activation by endogenous ligand. In *Cxcl12*$^{-/-}$ mice, almost all CXCR4 receptors were in the inactive state (Fig. 3Bb, lanes 3 and 4), suggesting that CXCL12 is the only CXCR4-activating ligand in the embryonic brain. Furthermore, CXCR4 signal was stronger in brain lysates (Fig. 3Bb, lanes 2 and 4; Fig. 3Bd, control versus *Cxcl12*$^{-/-}$) and cortical sections (Fig. 3Ca,c) from these mutants. Given that the level of *Cxcr4* mRNA was apparently unaltered in *Cxcl12* knockouts (Fig. 1Ca,b), these findings provide evidence that a substantial proportion of CXCR4 in the embryonic brain becomes downregulated after being activated by CXCL12.

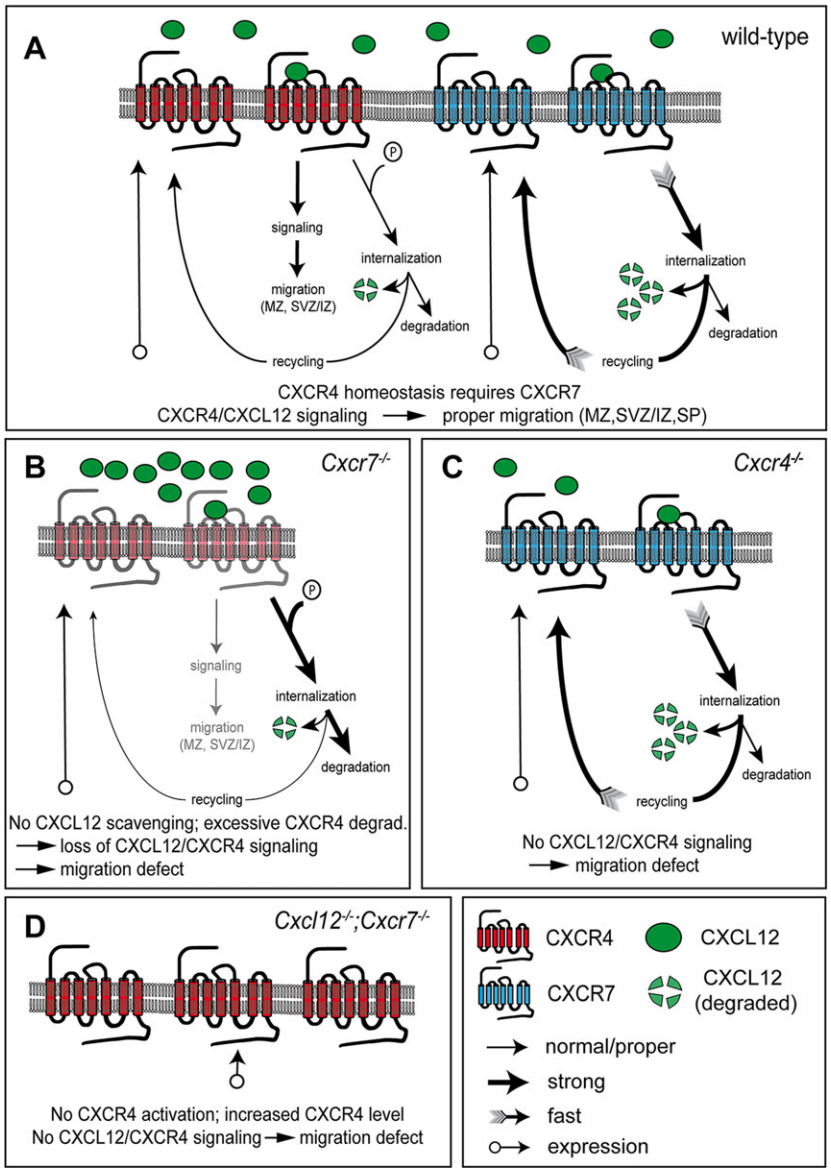

Fig. 4. Scheme illustrating functions of CXCR4 and CXCR7 in migrating cortical interneurons. (A) CXCL12 induces signaling and phosphorylation of CXCR4 as well as internalization of the CXCL12/CXCR4 complex. Internalized CXCR4 is recycled or degraded. CXCL12/CXCR4 signaling supports interneuron migration in the MZ and SVZ/IZ. Synthesis and degradation of CXCR4 are at equilibrium. CXCR7 mediates rapid internalization and degradation of CXCL12. (B) Absence of CXCR7 leads to extracellular CXCL12 accumulation and excessive CXCR4 activation and degradation. Loss of CXCR4 results in insufficient CXCL12/CXCR4 signaling and defective interneuron migration. (C) Lack of CXCL12/CXCR4 signaling causes defective interneuron migration. (D) The CXCR4 level is increased in the absence of CXCL12. CXCR7 deficiency does not cause excessive CXCR4 degradation because CXCR4 does not become phosphorylated when CXCL12 is not present. Lack of CXCL12/CXCR4 signaling causes defective interneuron migration.

Development (2014) 141, 1857-1863 doi:10.1242/dev.104224

As reported previously (Sánchez-Alcañiz et al., 2011), CXCR4 was hardly detectable in brain lysates and cortical sections from *Cxcr7*$^{-/-}$ mice (Fig. 3Ba, lanes 2 and 4; Fig. 3Bd, control group versus *Cxcr7*$^{-/-}$; Fig. 3Ca,b). We have now generated *Cxcl12*$^{-/-}$;*Cxcr7*$^{-/-}$ mice to test whether the loss of CXCR4 in *Cxcr7* mutants is mediated by CXCL12, and found that the activation state and expression level of CXCR4 in *Cxcl12*$^{-/-}$;*Cxcr7*$^{-/-}$ mice resembled those of *Cxcl12*$^{-/-}$ animals: almost all CXCR4 receptors were inactive (Fig. 3Bc, lanes 3 and 4) and the level of CXCR4 was increased compared with controls (Fig. 3Bc, lanes 2 and 4; Fig. 3Bd, control group versus *Cxcl12*$^{-/-}$;*Cxcr7*$^{-/-}$). CXCR4 immunostaining in the cortex was indistinguishable between *Cxcl12*$^{-/-}$;*Cxcr7*$^{-/-}$ and *Cxcl12*$^{-/-}$ mice: both cohorts showed a similar increase in CXCR4 signal as compared with the control (Fig. 3Ca,c,d) and a similar layering defect of CXCR4-immunoreactive neurons (supplementary material Fig. S3B).

Our findings in *Cxcr7*$^{-/-}$ and *Cxcl12*$^{-/-}$;*Cxcr7*$^{-/-}$ animals demonstrate that the embryonic brain contains sufficient CXCL12 to induce near complete CXCR4 degradation unless CXCR7-dependent scavenger activity prevents excessive CXCR4 activation by CXCL12. These findings and conclusions are summarized in Fig. 4.

MATERIALS AND METHODS

Animals and histochemistry

Animal procedures were in accordance with German and EU guidelines. Established mouse lines, *in situ* hybridization and immunohistochemical procedures, probes and antibodies were used (Memi et al., 2013; Stumm et al., 2002, 2003; Sánchez-Alcañiz et al., 2011). Transcripts from the *Neomycin* resistance cassette of *Cxcr4* mutants (Zou et al., 1998) were detected with a *Neo* probe cloned by PCR using *Cxcr4*$^{+/-}$ genomic DNA and 5′-ATGGGATCGGCCATTGAAC-3′ and 5′-TCAGAAG-AACTCGTCAAG-3′ primers.

CXCL12-565 uptake

Recombinant Atto565-tagged CXCL12 (CXCL12-565) (Yang et al., 1999) was labeled with a C-terminal ybbR13 tag (George et al., 2004; Zhou et al., 2007). Human embryonic kidney (HEK293) cells were transiently transfected as described (Hoffmann et al., 2012). Surface CXCR4 and CXCR7 receptors were immunostained in fixed non-permeabilized cells with N-terminal antibodies 2B11 (BD Biosciences) and 11G8 (Zabel et al., 2009), respectively. HEK293 cells and cortical slices were incubated with 20 nM CXCL12-565 at 37°C, washed, and fixed before confocal imaging.

Immunoblotting

Neuronal cultures (25×10^6 cells/dish) were prepared from E14.5 telencephalic vesicles and grown in Neurobasal medium/B27 supplement (Invitrogen). Compounds (20 nM CXCL12, Peprotech; 6 µM AMD3100, Sigma; 1 µM CCX771/CCX704, ChemoCentryx) were added 4 h after seeding in 6 ml fresh medium. Immunoblotting, detection and analysis were as described (Sánchez-Alcañiz et al., 2011).

Live cell imaging

Coronal brain slices (300 µm) were cut on a Vibratome (Leica), placed in 35 mm glass-bottom dishes (MatTek) and embedded in collagen (3 mg/ml, BD Biosciences). After adding DMEM lacking Phenol Red (Gibco), slices were transferred to the 37°C/5% CO_2 tissue incubation chamber attached to an LSM510 Meta inverted confocal microscope (Zeiss). The following live cell acquisition setup was used: EC Plan-Neofluor 20×/0.50 M27 objective, time series (interval: 10 min), *z*-stack acquisition, maximum intensity projection processing using Zen software (Zeiss). Statistical tests are specified in the figure legends (one, two and three symbols indicate $P\leq0.05$, $P\leq0.01$, and $P\leq0.001$, respectively).

Acknowledgements

We thank C. Anders, H. Bechmann, S. Bechmann and H. Stadler for excellent technical assistance and Dr Falko Nagel and Dr Stefan Schulz for providing UMB-2 antibody.

Competing interests

The authors declare no competing financial interests.

Author contributions

R.S., P.A. and W.M. designed the study. P.A., W.M. and D.S. carried out experiments, analyzed data and helped draft the manuscript. R.S. participated in data analysis and wrote the final manuscript. M.T., P.Z. and F.M. provided reagents and helped to establish the experiments.

Funding

The work was supported by the Deutsche Forschungsgemeinschaft (DFG) [grant STU 295/7-1].

Supplementary material

Supplementary material available online at
http://dev.biologists.org/lookup/suppl/doi:10.1242/dev.104224/-/DC1

References

Anderson, S. A., Eisenstat, D. D., Shi, L. and Rubenstein, J. L. R. (1997). Interneuron migration from basal forebrain to neocortex: dependence on Dlx genes. *Science* **278**, 474-476.

Balabanian, K., Lagane, B., Infantino, S., Chow, K. Y. C., Harriague, J., Moepps, B., Arenzana-Seisdedos, F., Thelen, M. and Bachelerie, F. (2005). The chemokine SDF-1/CXCL12 binds to and signals through the orphan receptor RDC1 in T lymphocytes. *J. Biol. Chem.* **280**, 35760-35766.

Bleul, C. C., Farzan, M., Choe, H., Parolin, C., Clark-Lewis, I., Sodroski, J. and Springer, T. A. (1996). The lymphocyte chemoattractant SDF-1 is a ligand for LESTR/fusin and blocks HIV-1 entry. *Nature* **382**, 829-833.

Boldajipour, B., Mahabaleshwar, H., Kardash, E., Reichman-Fried, M., Blaser, H., Minina, S., Wilson, D., Xu, Q. and Raz, E. (2008). Control of chemokine-guided cell migration by ligand sequestration. *Cell* **132**, 463-473.

Borrell, V. and Marín, O. (2006). Meninges control tangential migration of hem-derived Cajal-Retzius cells via CXCL12/CXCR4 signaling. *Nat. Neurosci.* **9**, 1284-1293.

Burns, J. M., Summers, B. C., Wang, Y., Melikian, A., Berahovich, R., Miao, Z., Penfold, M. E. T., Sunshine, M. J., Littman, D. R., Kuo, C. J. et al. (2006). A novel chemokine receptor for SDF-1 and I-TAC involved in cell survival, cell adhesion, and tumor development. *J. Exp. Med.* **203**, 2201-2213.

Cheng, Z.-J., Zhao, J., Sun, Y., Hu, W., Wu, Y. L., Cen, B., Wu, G. X. and Pei, G. (2000). beta-arrestin differentially regulates the chemokine receptor CXCR4-mediated signaling and receptor internalization, and this implicates multiple interaction sites between beta-arrestin and CXCR4. *J. Biol. Chem.* **275**, 2479-2485.

George, N., Pick, H., Vogel, H., Johnsson, N. and Johnsson, K. (2004). Specific labeling of cell surface proteins with chemically diverse compounds. *J. Am. Chem. Soc.* **126**, 8896-8897.

Hernández-Miranda, L. R., Parnavelas, J. G. and Chiara, F. (2010). Molecules and mechanisms involved in the generation and migration of cortical interneurons. *ASN Neuro.* **2**, e00031.

Hoffmann, F., Muller, W., Schutz, D., Penfold, M. E., Wong, Y. H., Schulz, S. and Stumm, R. (2012). Rapid uptake and degradation of CXCL12 depend on CXCR7 carboxyl-terminal serine/threonine residues. *J. Biol. Chem.* **287**, 28362-28377.

Jung, H., Bhangoo, S., Banisadr, G., Freitag, C., Ren, D., White, F. A. and Miller, R. J. (2009). Visualization of chemokine receptor activation in transgenic mice reveals peripheral activation of CCR2 receptors in states of neuropathic pain. *J. Neurosci.* **29**, 8051-8062.

Kalatskaya, I., Berchiche, Y. A., Gravel, S., Limberg, B. J., Rosenbaum, J. S. and Heveker, N. (2009). AMD3100 is a CXCR7 ligand with allosteric agonist properties. *Mol. Pharmacol.* **75**, 1240-1247.

Lewellis, S. W. and Knaut, H. (2012). Attractive guidance: how the chemokine SDF1/CXCL12 guides different cells to different locations. *Semin. Cell Dev. Biol.* **23**, 333-340.

Luker, K. E., Steele, J. M., Mihalko, L. A., Ray, P. and Luker, G. D. (2010). Constitutive and chemokine-dependent internalization and recycling of CXCR7 in breast cancer cells to degrade chemokine ligands. *Oncogene* **29**, 4599-4610.

Lysko, D. E., Putt, M. and Golden, J. A. (2011). SDF1 regulates leading process branching and speed of migrating interneurons. *J. Neurosci.* **31**, 1739-1745.

Marín, O. and Rubenstein, J. L. R. (2001). A long, remarkable journey: tangential migration in the telencephalon. *Nat. Rev. Neurosci.* **2**, 780-790.

Meechan, D. W., Tucker, E. S., Maynard, T. M. and LaMantia, A.-S. (2012). Cxcr4 regulation of interneuron migration is disrupted in 22q11.2 deletion syndrome. *Proc. Natl. Acad. Sci. U.S.A.* **109**, 18601-18606.

Memi, F., Abe, P., Cariboni, A., MacKay, F., Parnavelas, J. G. and Stumm, R. (2013). CXC chemokine receptor 7 (CXCR7) affects the migration of GnRH neurons by regulating CXCL12 availability. *J. Neurosci.* **33**, 17527-17537.

Miller, R. J., Banisadr, G. and Bhattacharyya, B. J. (2008). CXCR4 signaling in the regulation of stem cell migration and development. *J. Neuroimmunol.* **198**, 31-38.

Mueller, W., Schütz, D., Nagel, F., Schulz, S. and Stumm, R. (2013). Hierarchical organization of multi-site phosphorylation at the CXCR4 C terminus. *PLoS ONE* **8**, e64975.

Naumann, U., Cameroni, E., Pruenster, M., Mahabaleshwar, H., Raz, E., Zerwes, H.-G., Rot, A. and Thelen, M. (2010). CXCR7 functions as a scavenger for CXCL12 and CXCL11. *PLoS ONE* **5**, e9175.

Oberlin, E., Amara, A., Bachelerie, F., Bessia, C., Virelizier, J.-L., Arenzana-Seisdedos, F., Schwartz, O., Heard, J.-M., Clark-Lewis, I., Legler, D. F. et al. (1996). The CXC chemokine SDF-1 is the ligand for LESTR/fusin and prevents infection by T-cell-line-adapted HIV-1. *Nature* **382**, 833-835.

Paredes, M. F., Li, G., Berger, O., Baraban, S. C. and Pleasure, S. J. (2006). Stromal-derived factor-1 (CXCL12) regulates laminar position of Cajal-Retzius cells in normal and dysplastic brains. *J. Neurosci.* **26**, 9404-9412.

Rajagopal, S., Kim, J., Ahn, S., Craig, S., Lam, C. M., Gerard, N. P., Gerard, C. and Lefkowitz, R. J. (2010). Beta-arrestin- but not G protein-mediated signaling by the "decoy" receptor CXCR7. *Proc. Natl. Acad. Sci. U.S.A.* **107**, 628-632.

Sánchez-Alcañiz, J. A., Haege, S., Mueller, W., Pla, R., Mackay, F., Schulz, S., López-Bendito, G., Stumm, R. and Marín, O. (2011). Cxcr7 controls neuronal migration by regulating chemokine responsiveness. *Neuron* **69**, 77-90.

Schönemeier, B., Kolodziej, A., Schulz, S., Jacobs, S., Hoellt, V. and Stumm, R. (2008). Regional and cellular localization of the CXCl12/SDF-1 chemokine receptor CXCR7 in the developing and adult rat brain. *J. Comp. Neurol.* **510**, 207-220.

Sessa, A., Mao, C.-A., Colasante, G., Nini, A., Klein, W. H. and Broccoli, V. (2010). Tbr2-positive intermediate (basal) neuronal progenitors safeguard cerebral cortex expansion by controlling amplification of pallial glutamatergic neurons and attraction of subpallial GABAergic interneurons. *Genes Dev.* **24**, 1816-1826.

Stumm, R. and Hollt, V. (2007). CXC chemokine receptor 4 regulates neuronal migration and axonal pathfinding in the developing nervous system: implications for neuronal regeneration in the adult brain. *J. Mol. Endocrinol.* **38**, 377-382.

Stumm, R. K., Rummel, J., Junker, V., Culmsee, C., Pfeiffer, M., Krieglstein, J., Hollt, V. and Schulz, S. (2002). A dual role for the SDF-1/CXCR4 chemokine receptor system in adult brain: isoform-selective regulation of SDF-1 expression modulates CXCR4-dependent neuronal plasticity and cerebral leukocyte recruitment after focal ischemia. *J. Neurosci.* **22**, 5865-5878.

Stumm, R. K., Zhou, C., Ara, T., Lazarini, F., Dubois-Dalcq, M., Nagasawa, T., Hollt, V. and Schulz, S. (2003). CXCR4 regulates interneuron migration in the developing neocortex. *J. Neurosci.* **23**, 5123-5130.

Tanaka, D. H., Yanagida, M., Zhu, Y., Mikami, S., Nagasawa, T., Miyazaki, J.-i., Yanagawa, Y., Obata, K. and Murakami, F. (2009). Random walk behavior of migrating cortical interneurons in the marginal zone: time-lapse analysis in flat-mount cortex. *J. Neurosci.* **29**, 1300-1311.

Thelen, M. and Thelen, S. (2008). CXCR7, CXCR4 and CXCL12: an eccentric trio? *J. Neuroimmunol.* **198**, 9-13.

Tiveron, M.-C. and Cremer, H. (2008). CXCL12/CXCR4 signalling in neuronal cell migration. *Curr. Opin. Neurobiol.* **18**, 237-244.

Tiveron, M.-C., Rossel, M., Moepps, B., Zhang, Y. L., Seidenfaden, R., Favor, J., Konig, N. and Cremer, H. (2006). Molecular interaction between projection neuron precursors and invading interneurons via stromal-derived factor 1 (CXCL12)/CXCR4 signaling in the cortical subventricular zone/intermediate zone. *J. Neurosci.* **26**, 13273-13278.

Toritsuka, M., Kimoto, S., Muraki, K., Landek-Salgado, M. A., Yoshida, A., Yamamoto, N., Horiuchi, Y., Hiyama, H., Tajinda, K., Keni, N. et al. (2013). Deficits in microRNA-mediated Cxcr4/Cxcl12 signaling in neurodevelopmental deficits in a 22q11 deletion syndrome mouse model. *Proc. Natl. Acad. Sci. U.S.A.* **110**, 17552-17557.

Venkiteswaran, G., Lewellis, S. W., Wang, J., Reynolds, E., Nicholson, C., Knaut, H. et al. (2013). Generation and dynamics of an endogenous, self-generated signaling gradient across a migrating tissue. *Cell* **155**, 674-687.

Wang, Y., Li, G., Stanco, A., Long, J. E., Crawford, D., Potter, G. B., Pleasure, S. J., Behrens, T. and Rubenstein, J. L. R. (2011). CXCR4 and CXCR7 have distinct functions in regulating interneuron migration. *Neuron* **69**, 61-76.

Yang, O. O., Swanberg, S. L., Lu, Z., Dziejman, M., McCoy, J., Luster, A. D., Walker, B. D. and Herrmann, S. H. (1999). Enhanced inhibition of human immunodeficiency virus type 1 by Met-stromal-derived factor 1beta correlates with down-modulation of CXCR4. *J. Virol.* **73**, 4582-4589.

Zabel, B. A., Wang, Y., Lewen, S., Berahovich, R. D., Penfold, M. E. T., Zhang, P., Powers, J., Summers, B. C., Miao, Z., Zhao, B. et al. (2009). Elucidation of CXCR7-mediated signaling events and inhibition of CXCR4-mediated tumor cell transendothelial migration by CXCR7 ligands. *J. Immunol.* **183**, 3204-3211.

Zarbalis, K., Choe, Y., Siegenthaler, J. A., Orosco, L. A. and Pleasure, S. J. (2012). Meningeal defects alter the tangential migration of cortical interneurons in Foxc1hith/hith mice. *Neural Dev.* **7**, 2.

Zhou, Z., Cironi, P., Lin, A. J., Xu, Y., Hrvatin, S., Golan, D. E., Silver, P. A., Walsh, C. T. and Yin, J. (2007). Genetically encoded short peptide tags for orthogonal protein labeling by Sfp and AcpS phosphopantetheinyl transferases. *ACS Chem. Biol.* **2**, 337-346.

Zou, Y.-R., Kottmann, A. H., Kuroda, M., Taniuchi, I. and Littman, D. R. (1998). Function of the chemokine receptor CXCR4 in haematopoiesis and in cerebellar development. *Nature* **393**, 595-599.

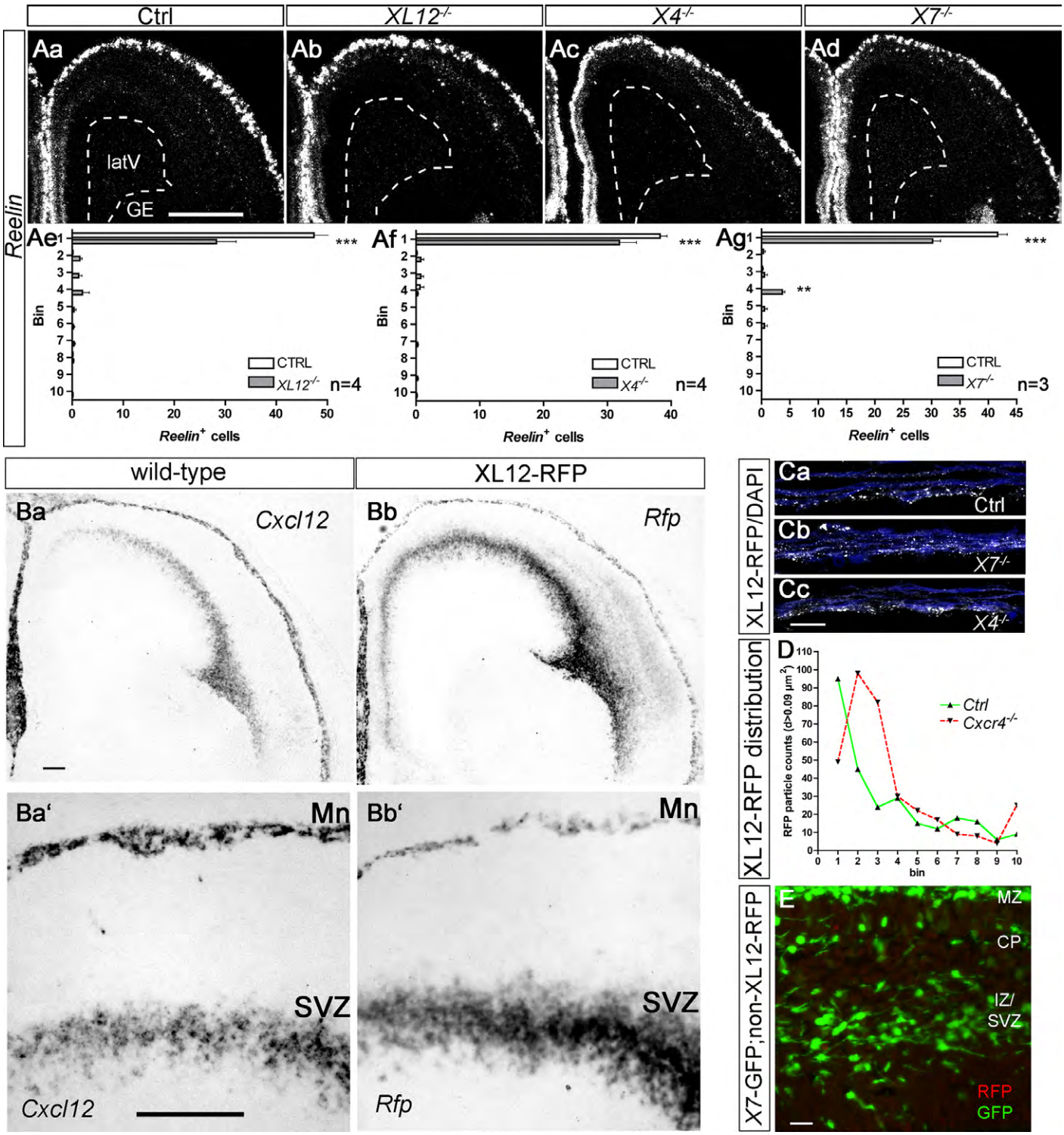

Supplemental Figure 1. Aa-Ad, Dark-field photographs of the dorsal telencephalon in emulsion-dipped coronal head sections after *in situ* hybridizations with a ^{35}S-labeled probe for *Reln* transcripts in control (Ctrl, Aa), *Cxcl12*$^{-/-}$ (*XL12*$^{-/-}$, Ab), *Cxcr4*$^{-/-}$ (*X4*$^{-/-}$, Ac), and *Cxcr7*$^{-/-}$ (*X7*$^{-/-}$, Ad) mice. **Ae-Ag**, Graphs show numbers of *Reln*$^{+}$ cells in 10 cortical bins (lateral cortex, see Figure 1 for counting scheme). Mutants were compared to control littermates using two-way ANOVA and Bonferroni´s post-hoc test (*Cxcl12*$^{-/-}$ and *Cxcr4*$^{-/-}$, n=4; *Cxcr7*$^{-/-}$, n=3). **Ba,Bb**, Bright-field photographs of the dorsal telencephalon in coronal head sections after *in situ* hybridizations with digoxigenin-labeled probes for *Cxcl12* and *Rfp* in a wild-type (Ba) and a CXCL12-RFP (Bb) mouse, respectively. **Ba´,Bb´**, Details of the cortex. *Cxcl12* and *Cxcl12-Rfp* transcripts exhibit similar patterns characterized by strong expression in the meninges and the subventricular/intermediate zone. **Ca-Cc**, Confocal images show immunostained RFP (white) in the meninges of E14.5 CXCL12-RFP (Ca, control), CXCL12-RFP;*Cxcr7*$^{-/-}$ (Cb, *X7*$^{-/-}$), and CXCL12-RFP;*Cxcr4*$^{-/-}$ (Cc, *X4*$^{-/-}$) mice. **D**, CXCL12-RFP signal distribution in E14.5 CXCL12-RFP (Ctrl) and CXCL12-RFP;*Cxcr4*$^{-/-}$ cortices. In the *Cxcr4* knockout the RFP signal shifts towards the CP/SP area (bins #2,3). **E,** Dual immunofluorescence for RFP/GFP in the cortex of an E14.5 *Cxcr7*-GFP mouse lacking the CXCL12-RFP transgene (non-XL12-RFP). RFP signal is absent in the overlay of the confocal RFP/GFP images. GE, ganglionic eminence; latV, lateral ventricle; Mn, meninges. Scale bars: Aa, 500 µm; Ba, Ba´, 200 µm; Cc,E, 20 µm.

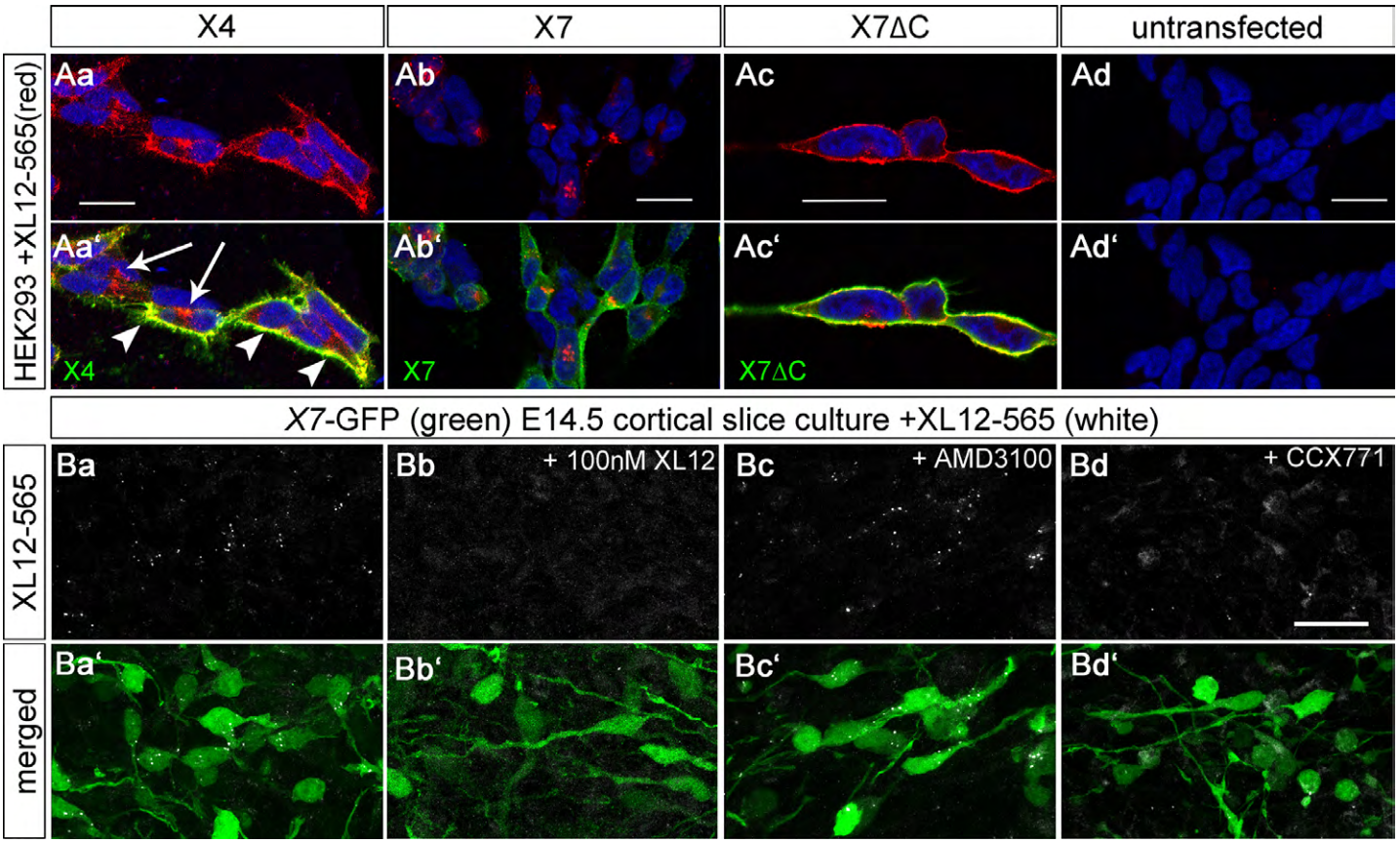

Supplemental Figure 2. A, Validation of CXCL12-565/receptor interaction. Transiently transfected HEK293 cells were incubated for 30 min at 37°C with CXCL12-565. Surface receptors were visualized in non-permeabilized cells with N-terminal antibodies (green). DAPI is shown in blue. **Aa**, In CXCR4-expressing cells (X4), most of the recovered CXCL12-565 (red) is colocalized with CXCR4 at the cell surface (arrowheads) and only a small fraction of the compound is internalized (arrow). **Ab**, In CXCR7-expressing cells (X7), virtually all of the recovered CXCL12-565 is clustered inside the cells. **Ac**, Transfectants of CXCR7ΔC (X7ΔC) that lacks the C-terminus and fails to internalize (Zabel et al., 2009) show CXCL12-565 exclusively at the cell surface. **Ad**, In untransfected cells, CXCL12-565 is not recovered. **Aa-Ad**, The images represent single confocal planes. It is concluded that CXCR7 rapidly internalizes CXCL12-565 whereas CXCR4 readily binds the compound but mediates less effective CXCL12-565 uptake than CXCR7. The qualitative results with CXCL12-565 correspond to quantitative results obtained with radiolabeled CXCL12 in a similar setting (Hoffmann et al., 2012). **B,** CXCL12-565 uptake in *Cxcr7*-GFP^{+} interneurons. Cortical slices from E14.5 *Cxcr7*-GFP (*X7*-GFP) transgenic embryos were incubated for 30 min at 37°C with CXCL12-565 and additional compounds as indicated. Native fluorescence, imaged by confocal microscopy, is shown for CXCL12-565 in white (Ba-Bd) and for CXCL12-565 plus GFP in the white/green overlay (Ba´-Bd´). Intracellular accumulation of CXCL12-565 in interneurons (Ba,Ba´) is blocked by excess non-fluorescent CXCL12 (XL12, Bb,Bb´) and the CXCR7 ligand CCX771 (Bd,Bd´), but not by the CXCR4 antagonist AMD3100 (Bc,Bc´).

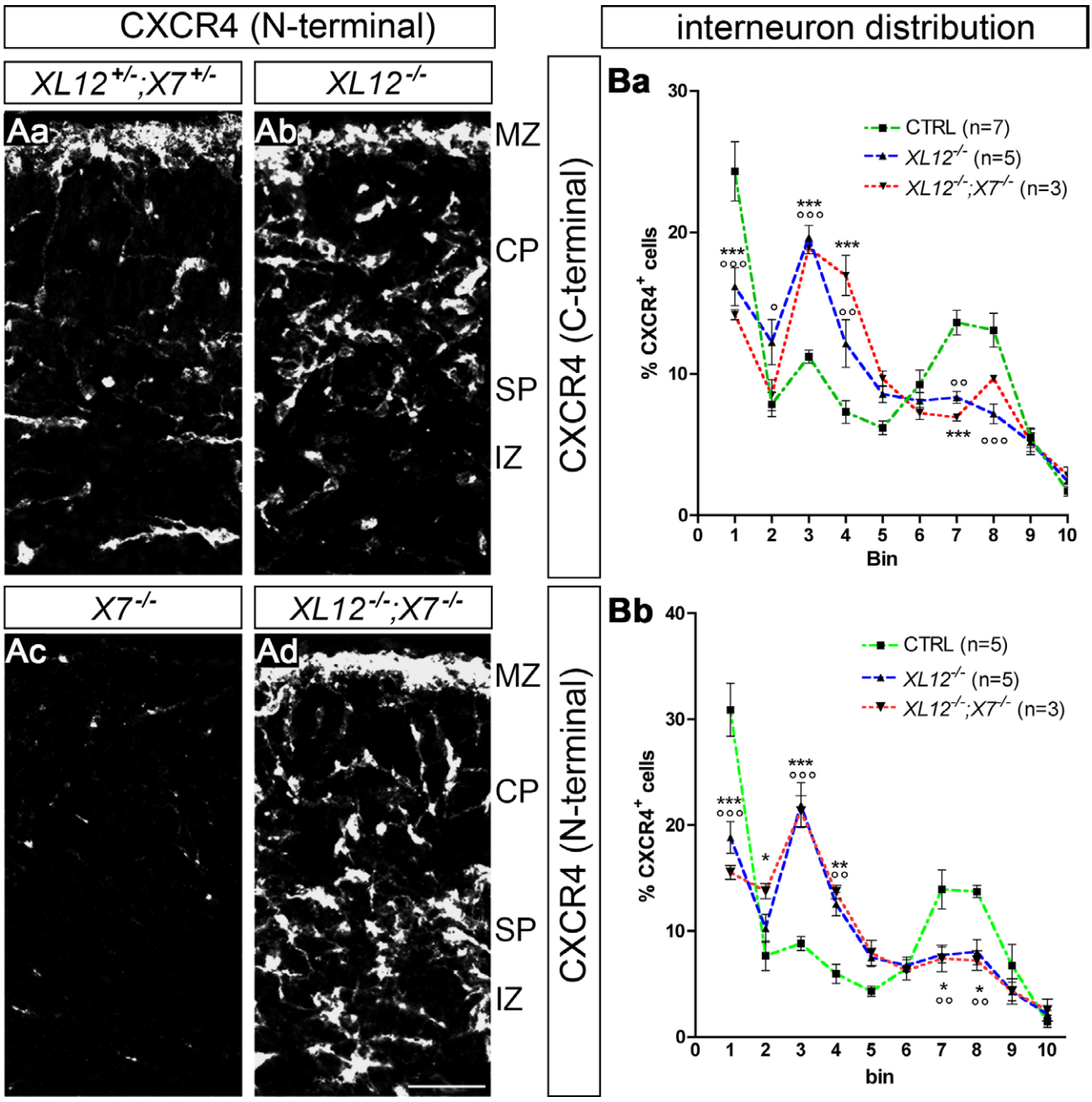

Supplemental Figure 3. Similar layering defect of CXCR4$^+$ cells in the cortex of E14.5 *Cxcl12*$^{-/-}$ and *Cxcl12*$^{-/-}$;*Cxcr7*$^{-/-}$ mice. A, CXCR4 was detected with phospho-insensitive N-terminal 2B11 antibody in coronal sections of an E14.5 litter (genotypes of littermates are specified in the Figure). **Ba,Bb,** UMB-2-immunoreactive cells (Ba) and 2B11-immunoreactive (Bb) were counted in 10 cortical bins in *Cxcl12*$^{-/-}$, *Cxcl12*$^{-/-}$;*Cxcr7*$^{-/-}$, and control mice (heterozygous or wild-type). Proportions per bin (% of all counted cells) are presented as mean±s.e.m. Mutants were compared to control mice using two-way ANOVA and Bonferroni´s post-test (^{o}*Cxcl12*$^{-/-}$; **Cxcl12*$^{-/-}$;*Cxcr7*$^{-/-}$). Note that abnormal layering of CXCR4$^+$ cells is similar in the two mutants. Scale bar in Ad: 50 µm.

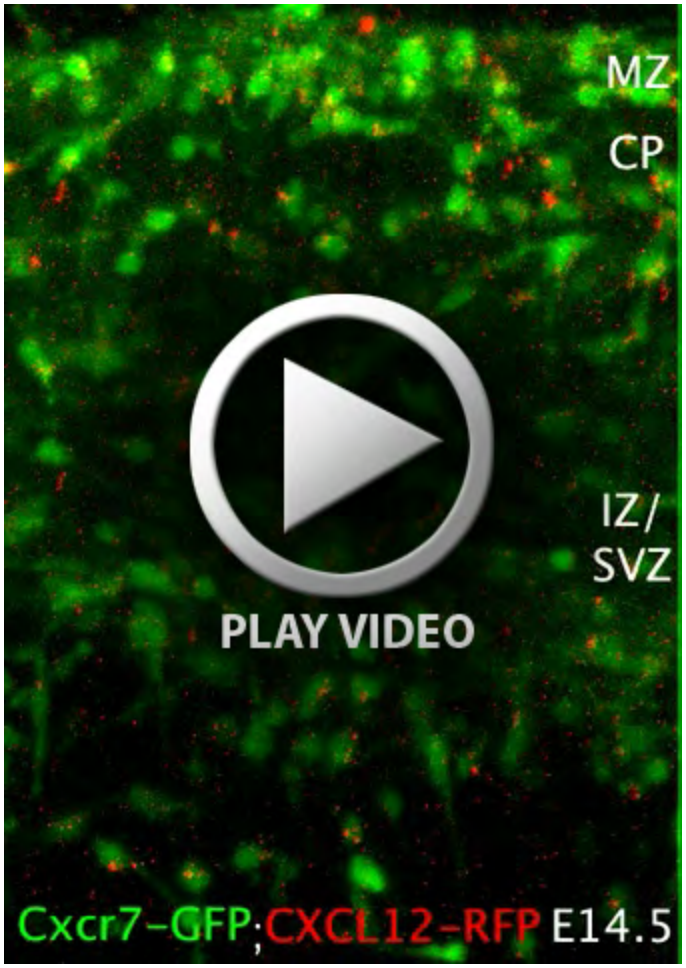

Movie 1. Virtually all *Cxcr7*$^{+}$ interneurons (96%) accumulate CXCL12-RFP while migrating through the cortex. Live cell imaging of *Cxcr7*-GFP;CXCL12-RFP double transgenic E14.5 embryo. Confocal image series of the lateral cortex (magnification: 200x; time: 15x10 min interval, z-stack: processed by maximum intensity projection with ZEN 2008 software). CP, cortical plate; IZ, intermediate zone; MZ, marginal zone; SVZ, subventricular zone.